A STUDY ON FIBER-ARRANGEMENT CLOSE TO THE ROOT OF A SHARP NOTCH, FOR SHORT FIBER-REINFORCED THERMOPLASTICS

R. Pietrogrande[1,2,*], M. De Monte[1], M. Quaresimin[2]

[1] Corporate Sector Research and Advance Engineering – Plastics Engineering (CR/APP2), Robert Bosch GmbH, 71272 Renningen, Germany, www.bosch.com

[2] University of Padova – Department of Management and Engineering, Stradella S. Nicola 3, 36100 Vicenza, Italy, www.unipd.it

[*] Riccardo.Pietrogrande@de.Bosch.com

Keywords: Short Fiber-Reinforced Thermoplastics, Notched specimen, Fiber-arrangement, Morphology

ABSTRACT

An approach, which aims at the morphological characterization near the sharp notch of specimens, has been developed for Short Fiber-Reinforced Thermoplastics. This work is directly related to the fatigue behavior of such materials, since the early stages of the cyclic damage are strictly influenced by the local microstructure at the stress concentration sites. Therefore, a comprehensive description of fibers' arrangement is needed in order to proceed with a modeling activity for the lifetime duration estimation. To this end, a semi-automatic tool has been developed, which is capable of evaluating fiber-arrangements through statistical descriptors, after submitting 2D pictures of the notch-tip area. Particularly, the attention was focused onto the nearest neighbor distance distribution function and onto a new formulation, which gives information about the level of the fiber-clustering phenomenon. On this basis, the repeatability of results has been evaluated with the goal of stating whether such information can be inherited by lifetime estimating models.

1 INTRODUCTION

In the last decades, short fiber-reinforced thermoplastics have been increasingly used in the automotive industry, for instance in the creation of parts for electrical and electronic equipment. Nowadays, the substitution of metallic parts through enhanced plastics is common practice. They provide not only outstanding mechanical properties but also offer large weight reduction possibilities. Furthermore, plastic parts can be produced with high efficiency and low cost, thanks to the advantage of injection molding technologies.

The fatigue behavior of such materials has not been completely explored yet and, to this end, different scientists have been developing failure criteria based on empirical [1], semi-empirical [2,3] and continuum mechanics [4,5] approaches. In all cases, it is possible to draw the conclusion that the damage, which occurs during fatigue cyclic loadings as well as the static response, is strongly depending on the spatial distribution of the fibers and on their orientation [1-6].

In literature, most of the information is referring to tests and experimental observations that are carried out on plain specimens [1-6]. Nevertheless, critical sites in components are usually located near a notch. Fiber orientation and spatial arrangement are highly dependent on the material flow. In this case, a sharp notch was created in a uniaxial specimen (figure 1) by means of a metallic slit directly inserted into the mold, which makes good simulative results about positioning of the fibers at this site difficult to obtain.

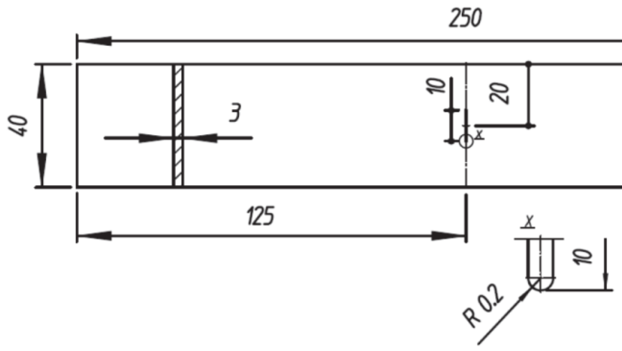

Figure 1: Sharply notched specimen. The isotropic k_t is equal to 9.8.

For PA66-GF materials, it has been demonstrated by Belmonte et al. [7] that fibers around a notch tip of uniaxial sharply notched specimens are preferentially oriented along the through-the-thickness direction and their level of clustering has a significant influence on the stress field within the matrix, which in turn drives the fatigue damage during the early stages (figure 2).

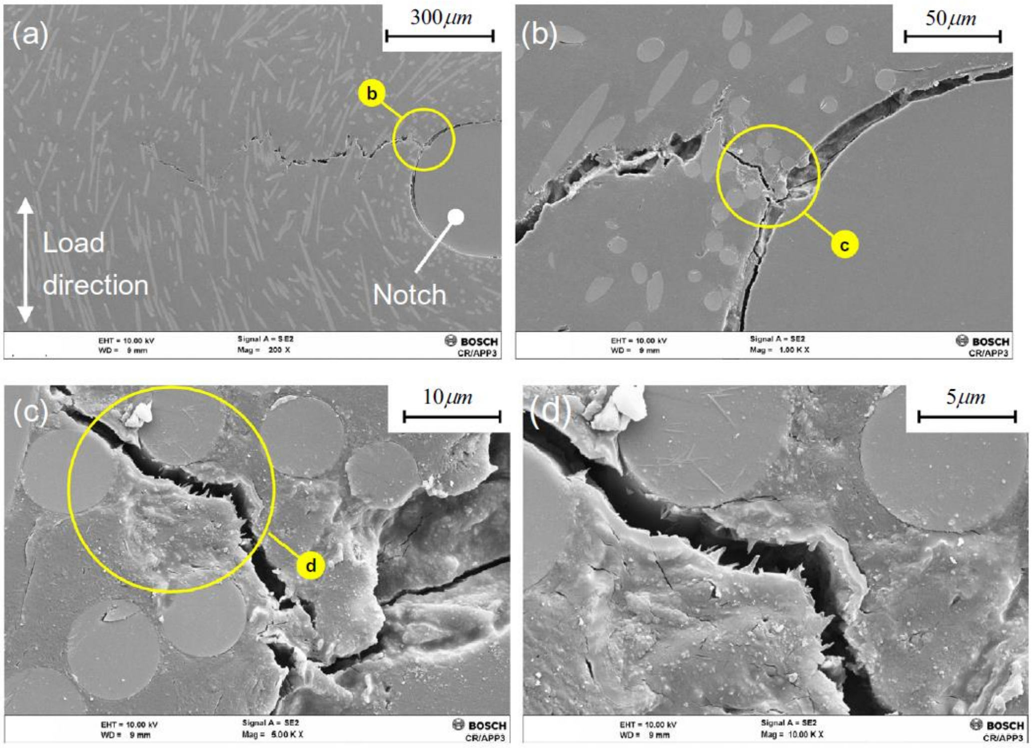

Figure 2: Fiber distribution at crack initiation for a notched specimen, interrupted fatigue tests. (b), (c) and (d) are magnified views of the crack [7].

2 DEVELOPMENT OF THE FIBER DETECTOR

In this context, the purpose of this work is to give a comprehensive statistical description of the fibers' morphology near the notch root. This is done for the case of sharply notched thermoplastic test specimens, which are reinforced with different contents of short glass fibers. The target of the study is to provide information that can be used at a later point for the virtual generation of the microstructure of a specific component.

To this purpose, a semi-automatic python-based tool has been created (figure 3), which, taking two dimensional pictures of the notch tip area as an input, is capable of evaluating the fibers arrangement by means of statistical descriptors. First of all, fibers that possess a through-the-thickness orientation can be marked manually. Secondly, different descriptors are adopted in order to evaluate the repeatability of the results among different pictures and materials. Fiber identification is done by separating the grey scale values. The nearest neighbor fiber distribution is then plotted to assess the lowest distance that can occur between fibers around the notch [8-10]. Furthermore, the Ripley's K function [8,9] usage has been considered for clusters quantification. Since this function is suitable only for large or periodic (in the case of RVEs) observation areas [9], a modification of it has been proposed to establish the level of cluster formation. Furthermore, the modified Ripley's function is used to compute a significant length, which is identified as the maximum distance between fibers within a cluster. After isolating clusters, consideration on their size and on their amount can be done.

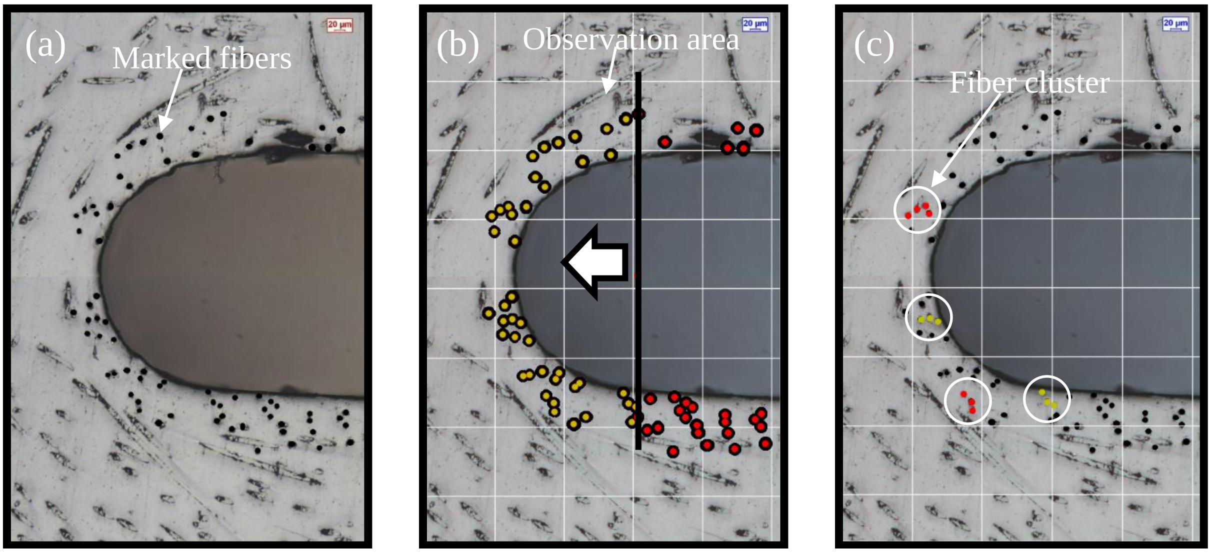

Figure 3: Working principle of the tool for detecting fibers' position. In (a) manually marked fibers are shown, in (b) they are automatically detected by the tool and in (c) fiber clusters are isolated.

3 RESULTS

In this section, some images of two different materials have been submitted to the tool in order to analyse the distribution of fibers around the notch and to assess whether clusters can be detected.

First of all, a statistical description of the 2D morphology for a PA66-GF15 has been carried out. With regards to the nearest neighbor distribution function, a certain repeatability is encountered (figure 4).

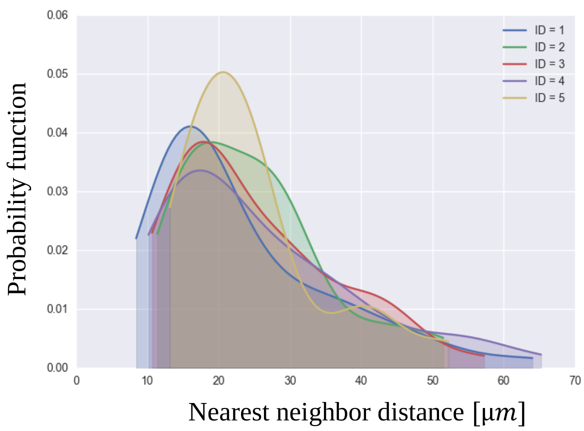

Figure 4: Nearest neighbor distribution function. Example for five pictures (identified with ID), for the case of PA66-GF15 specimens. The observation area is the same as in figure 3.

It can be observed that for different observed pictures the most occurring minimum distance between fiber centers is within the range 15÷20 μm. The following function is then proposed in order to establish the maximum fiber-relative distance which could identify a cluster.

$$\rho_f = \sum_i \sum_{j \neq i} \frac{I\left(d_{ij} \leq r_i\right)}{A_i} \tag{1}$$

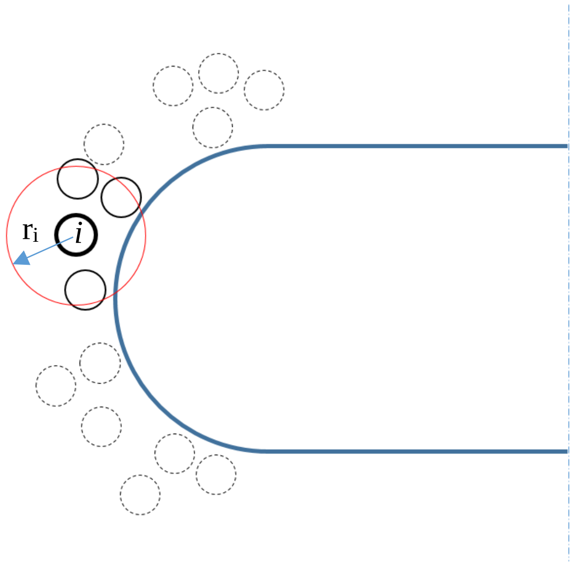

Figure 5: Parameters for the proposed function definition.

Referring to expression 1 and to figure 5, A_i stands for the area of the circle centered in the i-th fiber. d_{ij} is the distance between j-th and the the i-th and $I(d_{ij} \leq r_{ij})$ is equal to 1 whether the j-th fiber center is within the circumference with radius r_i and equal to 0 in the opposite case. By plotting the proposed function, figure 6 is then obtained.

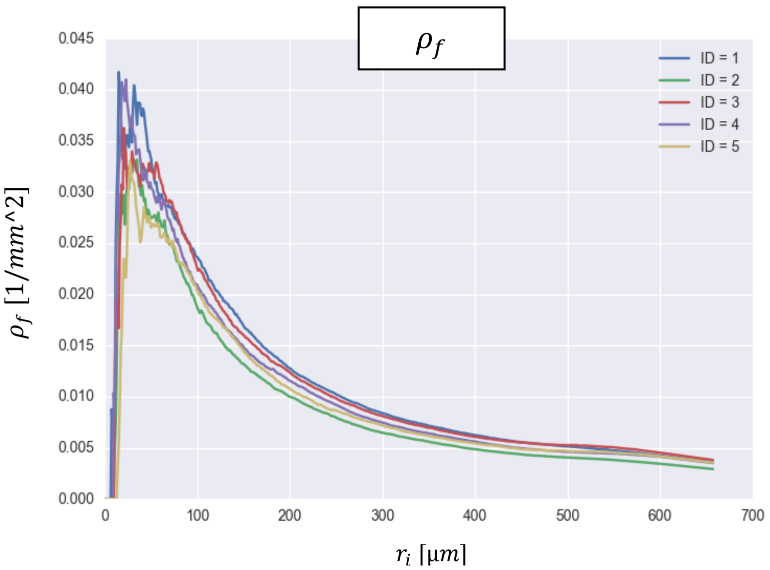

Figure 6. Proposed function plot for PA66-GF15 specimens (example for 5 pictures identified with their own ID).

A maximum of the functions can be identified. Furthermore, it can be used for the proposed fiber-cluster detector as the maximum distance between fibers that establishes a fiber cluster. Looking at figure 5, a value of 25 µm can be chosen since the maximum of the functions lays within 15 and 30 µm.

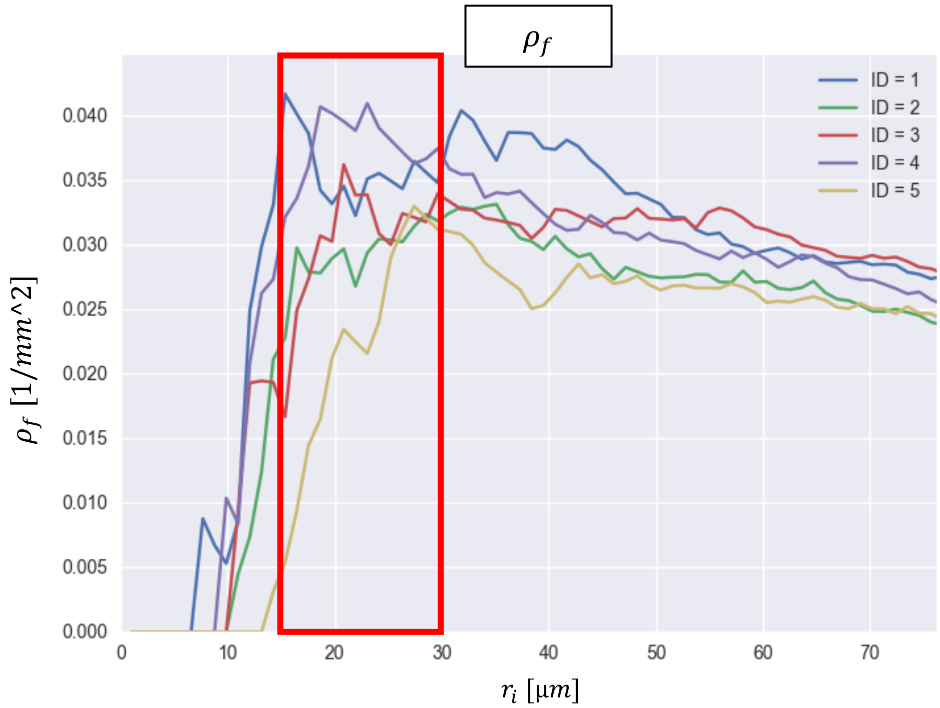

Figure 7: Zoom of figure 6 around the maximum values.

After isolating fiber-clusters, as it is shown in figure 3, some considerations can be done. For instance, for the set of analyzed pictures it can be stated that the amount of clusters around the notch-root is 3-4 (figure 8).

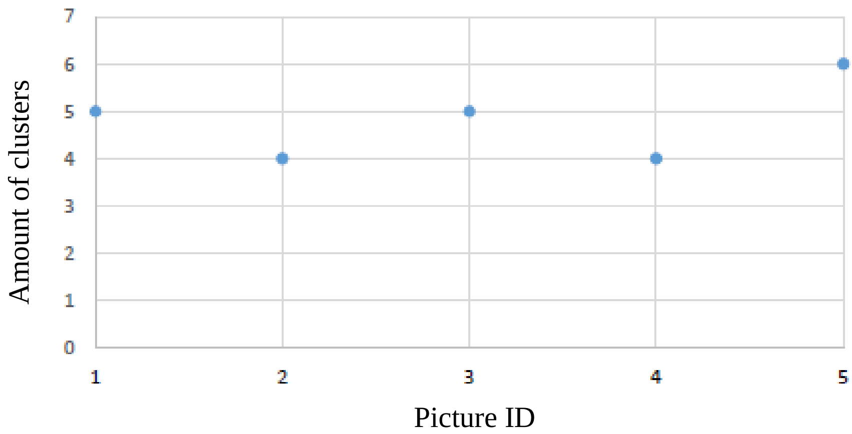

Figure 8: Amount of fiber-clusters for PA66-GF15.

The size of these clusters respects a certain repeatability as well, being mostly composed of 3-4 fibers each (figure 9).

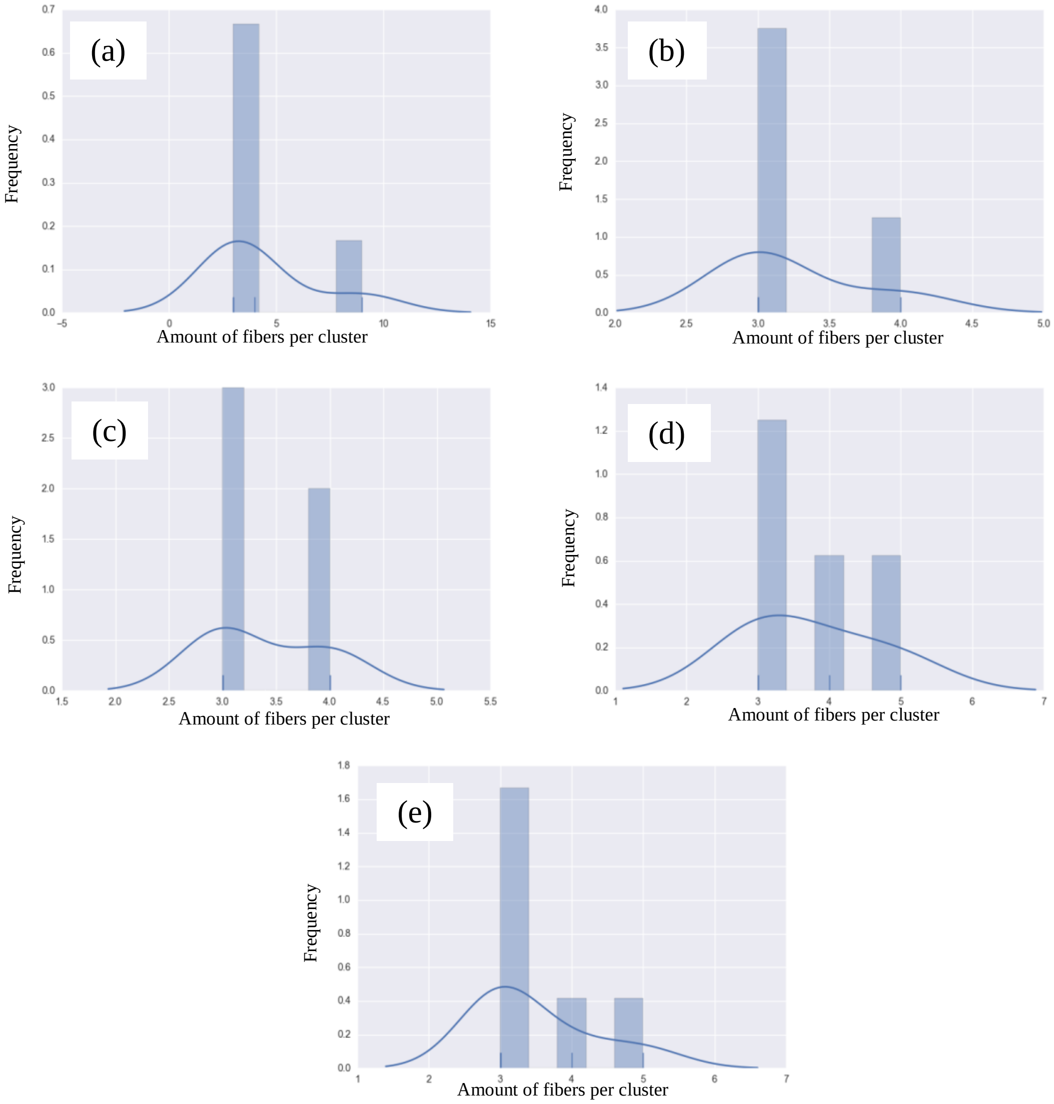

Figure 9: Clusters' size for PA66-GF15.

The same procedure has been applied to the case of PA66-GF35 (35% of fiber-mass). The results regarding the *nearest neighbor distribution function* are therefore the followings:

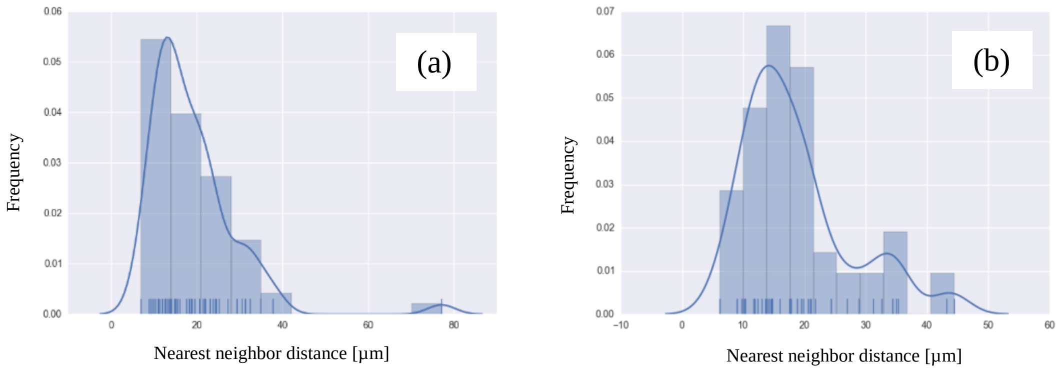

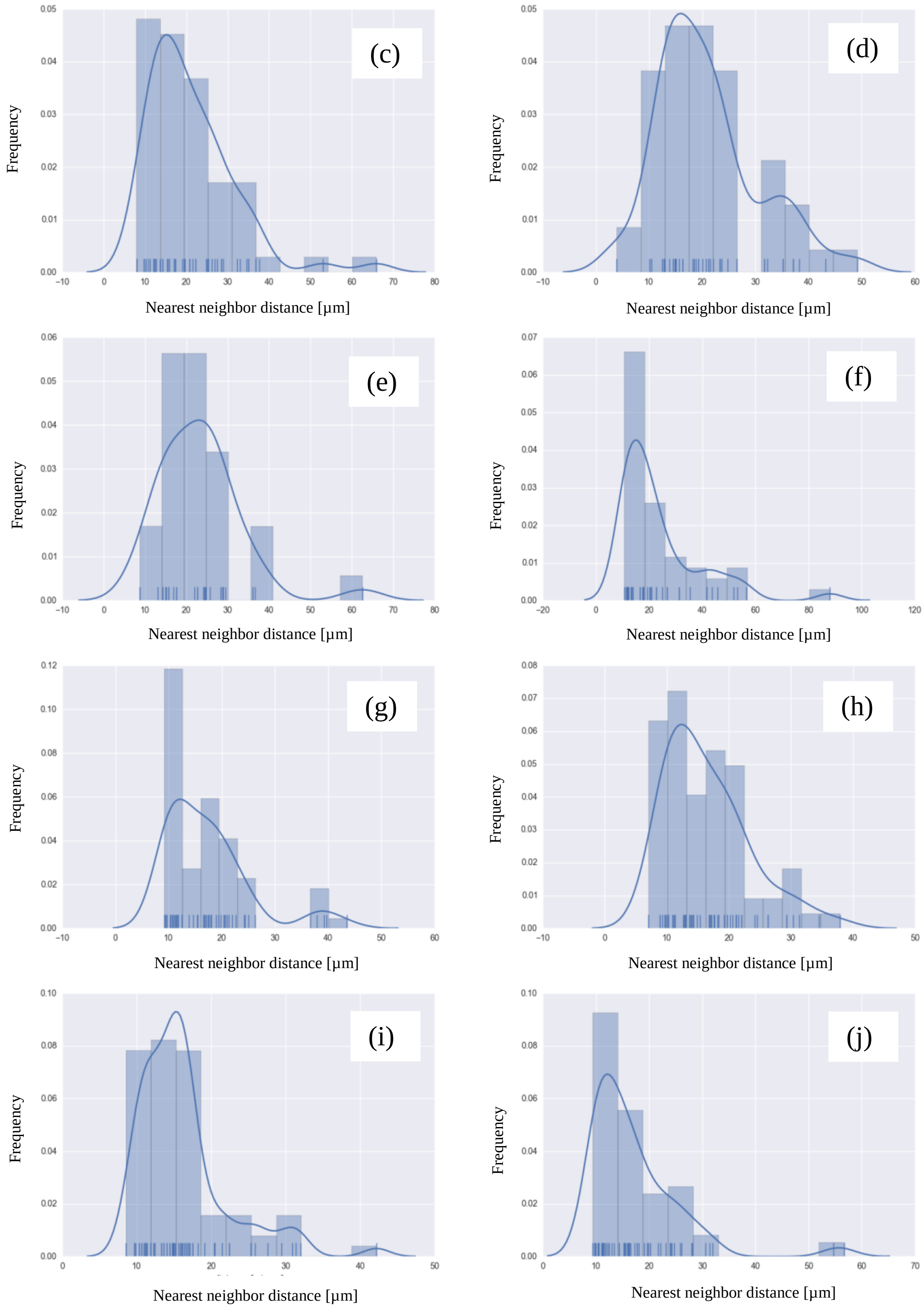
(c)
(d)
(e)
(f)
(g)
(h)
(i)
(j)
Frequency
Nearest neighbor distance [μm]

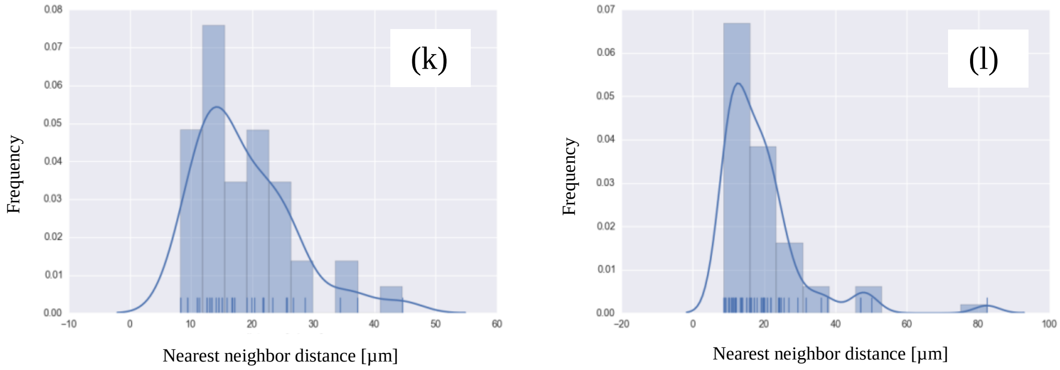

Figure 10: Nearest neighbor distribution function for PA66-GF35.

From figure 10, it can be clearly concluded that the most repeated nearest fiber-distance is within the interval 15÷20 µm, similarly to the case of PA66-GF15.

Concerning the proposed function 1, the trend of it seems to respect the same that has been encountered for PA66-GF15: the complete function of one analyzed images for a PA66-GF35 specimen is reported in figure 11 as an example.

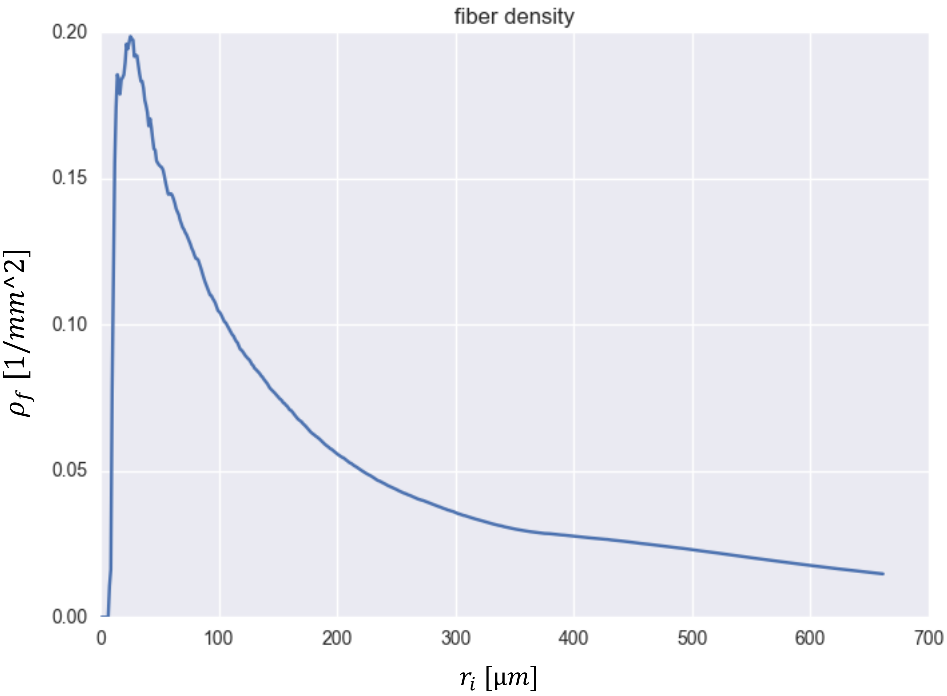

Figure 11: Example of plot of the ρ_f function for PA66-GF35.

Particularly, figure 12 zooms onto the peaks of ρ_f corresponding to the same specimens as figure 10.

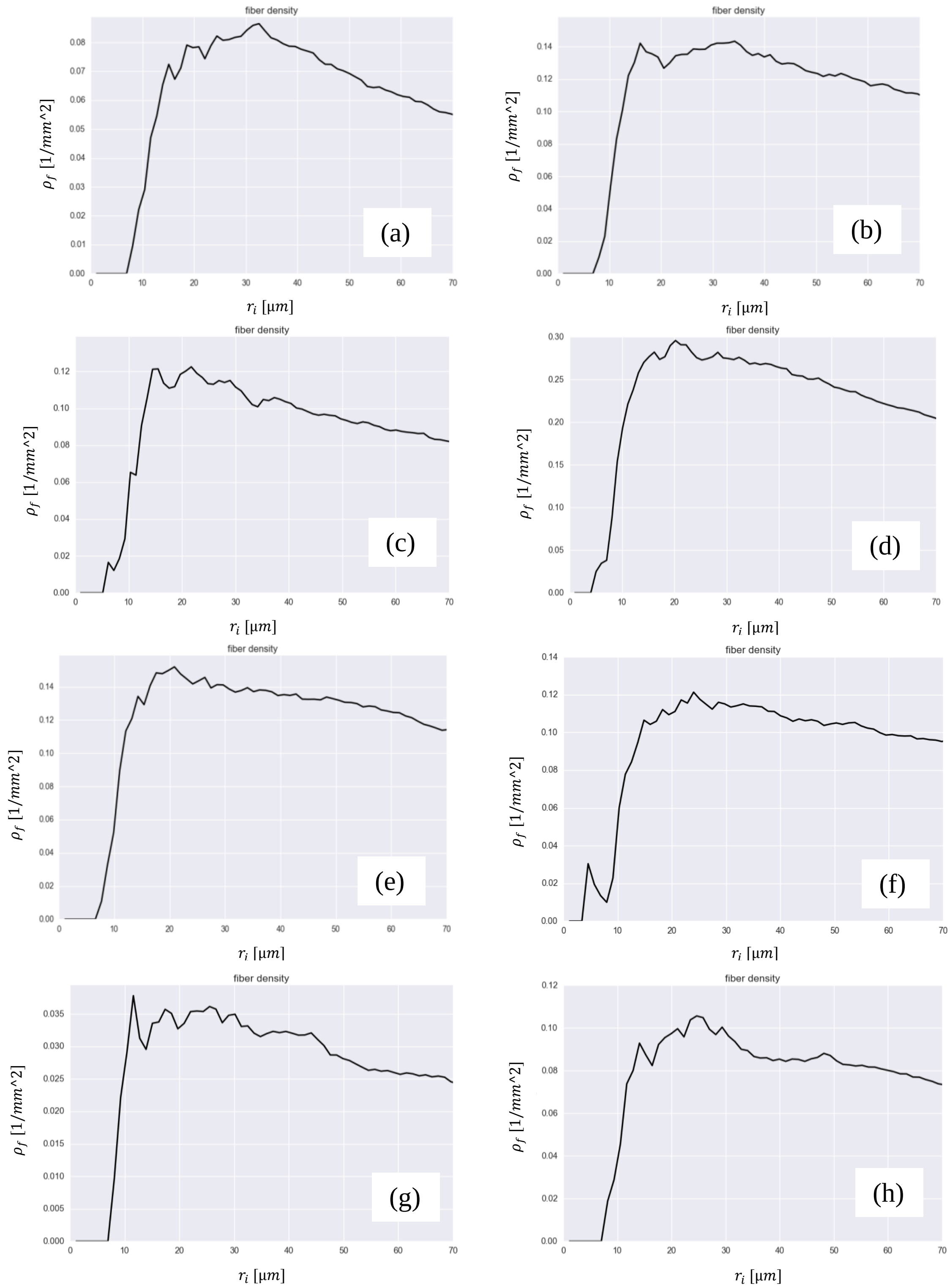
fiber density
ρ_f [1/mm^2]
r_i [μm]
(a)
(b)
(c)
(d)
(e)
(f)
(g)
(h)

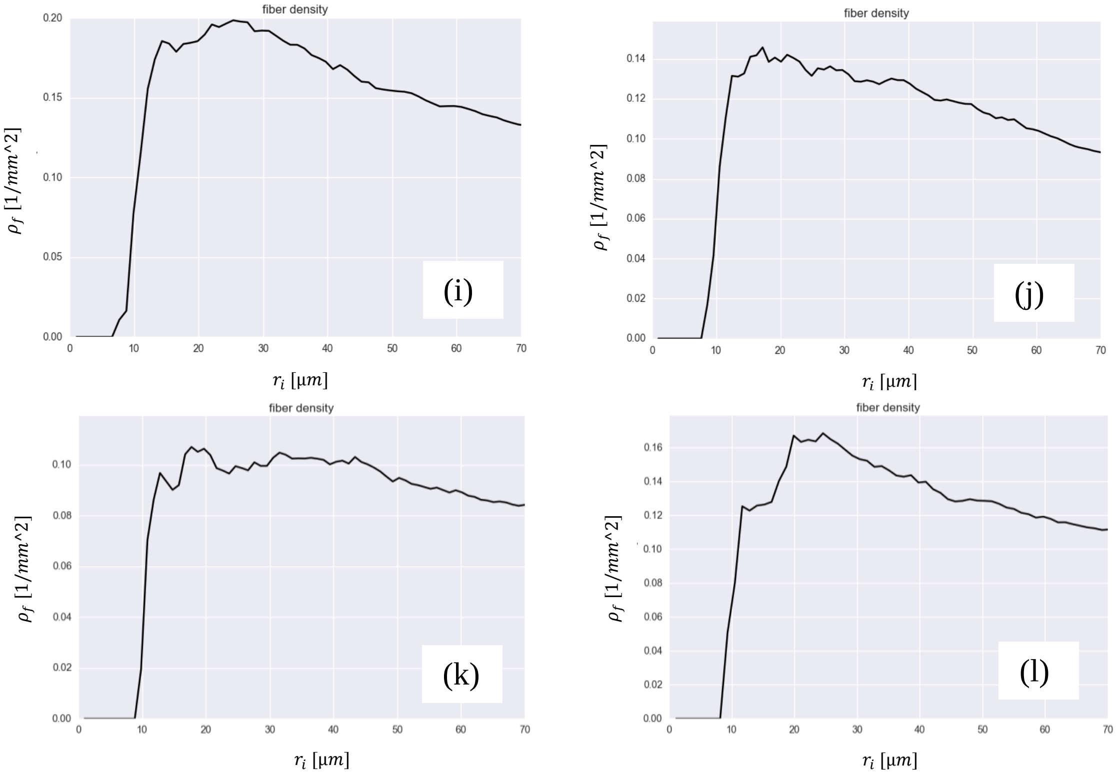

Figure 12: Zoom on the peaks of the ρ_f for PA66-GF35.

Observing figure 12, the peak of the function has a good repeatability and the most frequent value along the *x*-axis is within the range 15÷30 µm, as it was observed for the former material. The value of 25 µm could been used again as maximum distance between fibers for clusters' definition sake, but for such a high volume fraction, fibers are better distributed around the notch and a clear formation of clusters cannot be stated (figure 13).

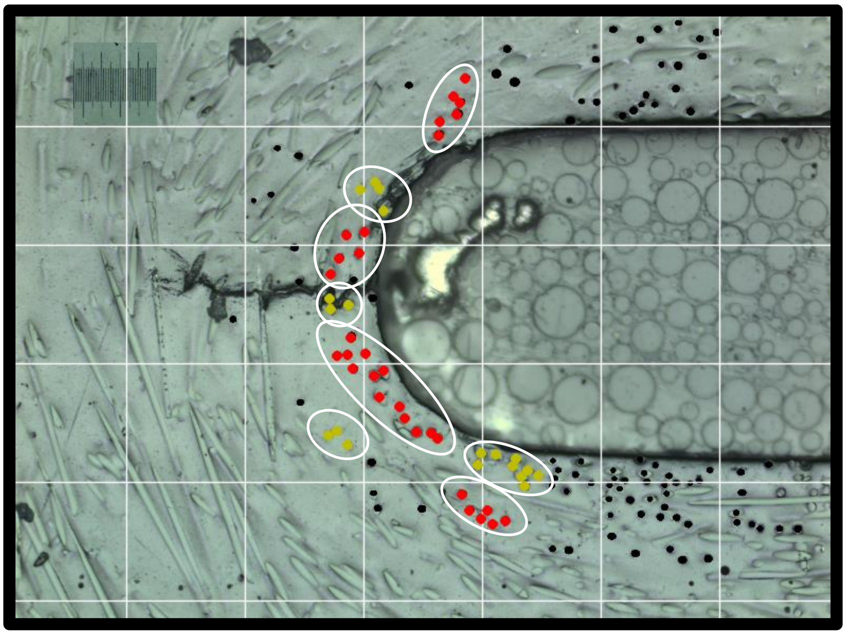

Figure 13: Example of cluster detection for PA66-GF35. Due to the large amount of fibers, it is not possible to well separate fiber-clusters.

4 CONCLUSION

The aim of this work was to provide a new methodology for the description of the 2D fiber-arrangement in the case of sharply notched reinforced thermoplastics. The *nearest neighbour fiber distribution function* has been adopted, demonstrating a good statistical repeatability for two different materials: PA66-GF15 and PA66-GF35. Afterwards, a function which is derived from the modification of the Ripley's K function has been formulated and applied to the considered cases. Also in this case, the repeatability has been fulfilled with regards to the position of the peak along the *x*-axis. Concerning the position of it along the *y*-axis, the material with 35 wt% yields higher values compared to the 15 wt% material, as it is expected, since the proposed function provides a measurement of the local fiber density.

Eventually, it can be established that for high fiber volume fractions the detection of fiber-clusters is hindered by the large amount of inclusions that surround the notch.

REFERENCES

[1] M.F. Arif, “Damage mechanisms in short glass fiber reinforced polyamide-66 under monotonic and fatigue loading: Effect of the relative humidity and injection molding induced microstructure”, *PhD Thesis* (2014).

[2] M. De Monte, “Multiaxial fatigue behaviour of short fibre reinforced thermoplastics”, PhD Thesis, ISBN 978-3-00-023988-5 (2008).

[3] A. Bernasconi, P. Davoli, A. Basile, A. Filippi, “Effect of fiber orientation on the fatigue behaviour of a short glass fibre reinforced polyamide-6”, International journal of Fatigue, 29, 199-208, (2007).

[4] H. Nouri, F. Meraghni, P. Lory, “Fatigue damage model for injection-molded short fibre reinforced thermoplastics”, International Journal of Fatigue, 31, 934-942 (2009).

[5] H. Nouri, C. Czarnota, F. Meraghni, “Experimental Parameter identification of fatigue damage model for short reinforced thermoplastics GFRP”, Design and Modeling of Mechanical Systems, Proceeding of the fifth international conference on design and modeling of mechanical systems, CMSM’2013, Djerba, Tunisia (2013).

[6] M. De Monte, E. Moosbrugger, M. Quaresimin, “Influence of temperature and thickness on the off-axis behaviour of short glass fibre reinforced polyamide 6.6 – cyclic loading”, Composite: Part A, 41, 1368-1379 (2010).

[7] E. Belmonte, M. De Monte, C.J. Hoffmann, M. Quaresimin, “Damage mechanisms in a short glass fiber reinforced polyamide under fatigue loading”, International Journal of Fatigue, 94, 145-157 (2017).

[8] A.R. Melro, P.P Camanho, S.T. Pinho, “Generation of random distribution of fibres in long-fibre reinforced composites”, Composite Science and Technology, 68, 2092-2102 (2008).

[9] V. Romanov, S.V. Lomov, Y. Swolfs, S. Orlova, L. Gorbatikh, I. Verpoest, “Statistical analysis of real and simulated fibre arrangments in unidirectional composites”, Composite Science and Technology, 87, 126-134 (2013).

[10] Y. Ismail, D. Yang, J. Ye, “Discrete element method for generating random fibre distributions in micromechanical models of fibre reinforced composite laminates”, Composites Part B, 90, 485-492.